

RESEARCH LETTER

10.1002/2016GL069465

Key Points:

- CMIP5 precipitation biases have significant hemispherically symmetric and antisymmetric components
- Hemispherically antisymmetric biases are related to the cross-equatorial atmospheric energy flux
- Hemispherically symmetric biases are related to the atmospheric net energy input near the equator

Supporting Information:

- Supporting Information S1
- Figure S1
- Figure S2

Correspondence to:

O. Adam,
ori.adam@live.com

Citation:

Adam, O., T. Schneider, F. Brient, and T. Bischoff (2016), Relation of the double-ITCZ bias to the atmospheric energy budget in climate models, *Geophys. Res. Lett.*, 43, 7670–7677, doi:10.1002/2016GL069465.

Received 5 MAY 2016

Accepted 17 JUN 2016

Accepted article online 24 JUN 2016

Published online 18 JUL 2016

Relation of the double-ITCZ bias to the atmospheric energy budget in climate models

Ori Adam¹, Tapio Schneider^{1,2}, Florent Brient¹, and Tobias Bischoff²
¹Department of Earth Sciences, ETH Zurich, Zurich, Switzerland, ²California Institute of Technology, Pasadena, California, USA

Abstract We examine how tropical zonal mean precipitation biases in current climate models relate to the atmospheric energy budget. Both hemispherically symmetric and antisymmetric tropical precipitation biases contribute to the well-known double-Intertropical Convergence Zone (ITCZ) bias; however, they have distinct signatures in the energy budget. Hemispherically symmetric biases in tropical precipitation are proportional to biases in the equatorial net energy input; hemispherically antisymmetric biases are proportional to the atmospheric energy transport across the equator. Both relations can be understood within the framework of recently developed theories. Atmospheric net energy input biases in the deep tropics shape both the symmetric and antisymmetric components of the double-ITCZ bias. Potential causes of these energetic biases and their variation across climate models are discussed.

1. Introduction

Most current coupled general circulation models overestimate precipitation over oceans in the southern tropics and underestimate it in the equatorial Pacific (Figure 1a) [e.g., Lin, 2007; Li and Xie, 2014]. This problem is called the double-Intertropical Convergence Zone (ITCZ) bias because the ITCZ in the models splits into two rainbands more often than is observed. The double-ITCZ bias dates back to the earliest climate models [Mehchoo et al., 1995] and, despite substantial advances in climate modeling, persists in the current climate models that participated in phase 5 of the Climate Model Intercomparison Project (CMIP5) [Li and Xie, 2014; Zhang et al., 2015; Tian, 2015].

Because the ITCZ can change in response to distant perturbations in the energy budget, for example, in high latitudes [e.g., Vellinga and Wood, 2002; Chiang and Bitz, 2005; Broccoli et al., 2006; Kang et al., 2008; Chiang and Friedman, 2012; Schneider et al., 2014], the causes of the double-ITCZ bias may lie in distant biases in the atmospheric energy budget. For example, biases in the representation of extratropical clouds over the Southern Ocean have been suggested to cause the double-ITCZ bias [Hwang and Frierson, 2013]. But climate models also exhibit biases in the tropical atmospheric energy budget, which can likewise affect the double-ITCZ bias. For example, CMIP5 models produce overly bright low-level clouds in the tropics, and they misrepresent the distribution of these clouds [e.g., Nam et al., 2012]. Such biases in the radiative energy budget can affect the tropical precipitation distribution [e.g., Philander et al., 1996; Li and Xie, 2012]. Or biases in ocean dynamics, such as unresolved ocean eddy fluxes [e.g., Abernathy and Wortham, 2015] and unrealistic coastal upwelling [e.g., Delworth et al., 2012; Small et al., 2014], can lead to biases in ocean energy uptake. Such biases in ocean energy uptake can likewise affect the tropical precipitation distribution and may lead to a double-ITCZ bias [Bischoff and Schneider, 2014; Schneider et al., 2014; Bischoff and Schneider, 2016]. The persistence of the double-ITCZ bias across generations of climate models has its roots in our inability so far to link the ITCZ bias mechanistically to biases in the representation of atmospheric and oceanic processes. The highly interactive nature of the Earth system exacerbates this difficulty. This paper identifies potential causes of the double-ITCZ bias by examining its relation to energetic biases both in the tropics and in the extratropics.

Broccoli et al. [2006], Kang et al. [2008], and Donohoe et al. [2013], among others, have shown that the ITCZ shifts southward as the northward atmospheric energy transport (AET) across the equator strengthens and conversely as it weakens. In the present climate, the mean position of the marine ITCZ at 6°N (Figure 1a) is associated with a southward energy flux across the equator of about 0.2 PW (1 PW = 10¹⁵ W)—a result of the Northern Hemisphere (NH) being warmer than the Southern Hemisphere (SH) because of northward ocean energy transport in the Atlantic [e.g., Marshall et al., 2014].

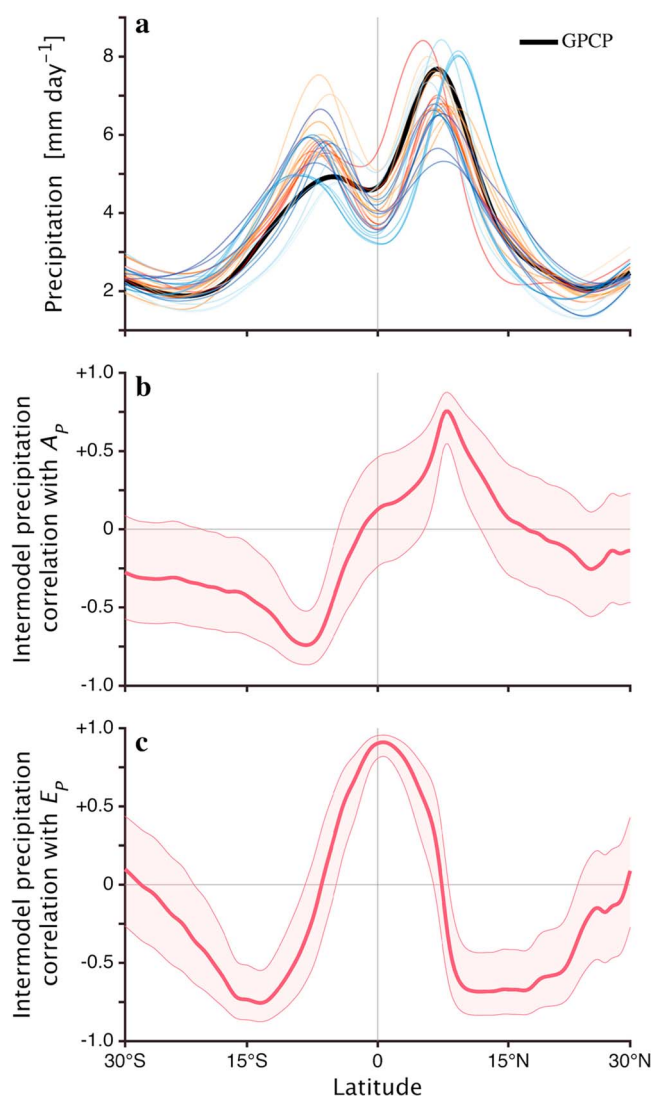


Figure 1. (a) Climatological (1979–2004) annual mean and zonal mean precipitation according to the GPCP data set (black) and CMIP5 models (colors). (b) Meridional dependence of the (Pearson) correlation coefficient between the tropical precipitation asymmetry index A_p and the annual mean and zonal mean precipitation in CMIP5 models. Shading indicates 95% confidence bounds calculated using t statistics. (c) As in Figure 1b but showing the correlation with the equatorial precipitation index E_p .

2. Methods and Data

2.1. Theory

The zonally averaged and column-integrated meridional energy transport in the atmosphere vanishes near the ITCZ, so the ITCZ can be roughly associated with the atmospheric “energy flux equator” [e.g., Kang *et al.*, 2008; Donohoe *et al.*, 2013; Adam *et al.*, 2016]. Approximate expressions for the energy flux equator (EFE) can be obtained as zeros of the zonally averaged and column-integrated meridional energy flux in the atmosphere, Taylor expanded in latitude near the equator (see the supporting information). To first order, the location of the EFE (roughly the ITCZ position) can be approximated by [Bischoff and Schneider, 2014]

$$\phi_{\text{EFE}} = -\frac{1}{a} \frac{\text{AET}_0}{\text{NEI}_0}, \quad (1)$$

where ϕ denotes latitude, a is Earth’s radius, and AET_0 and NEI_0 denote the atmospheric energy transport and equatorial net energy input at the equator.

The double-ITCZ bias in climate models implies an overall southward shift of the precipitation distribution, whose magnitude in models has been shown to be correlated with biases in the cross-equatorial AET [Hwang and Frierson, 2013]. This overall southward shift is a hemispherically asymmetric bias in the tropical precipitation distribution. Recent theoretical advances linking the ITCZ position to the atmospheric energy budget suggest that hemispheric energy budget biases in the tropical precipitation distribution—e.g., a double ITCZ straddling the equator symmetrically instead of a single ITCZ on the equator—may arise through biases in the net energy input (NEI) to the atmosphere near the equator [Bischoff and Schneider, 2014, 2016]. Therefore, it can be fruitful to analyze the hemispherically symmetric and antisymmetric components of the tropical precipitation distribution separately and relate biases in them to the atmospheric energy budget. This is the approach we pursue in the present paper.

We analyze the annual mean and zonal mean precipitation distribution and atmospheric energy budget of CMIP5 historical simulations (with coupled models driven by prescribed atmospheric compositions) and compare them with observations. The data and methods underlying our analysis are presented in section 2. The hemispherically symmetric and antisymmetric components of biases and intermodel variations are examined in section 3. The processes that may be responsible for the biases are discussed in section 4.

According to equation (1), changes in AET_0 at fixed NEI_0 lead to meridional shifts of the ITCZ, which are generally asymmetric about the equator. To the extent precipitation variations associated with ITCZ shifts follow the ITCZ position (e.g., if the precipitation distribution around the ITCZ remains invariant during the ITCZ shifts), precipitation variations associated with variations in AET_0 therefore generally have a hemispherically antisymmetric component. Conversely, changes in NEI_0 at fixed AET_0 lead to shifts of the ITCZ toward or away from the equator. If the mean ITCZ position is off the equator, variations in NEI_0 can then again lead to asymmetric precipitation variations. However, if the ITCZ symmetrically shifts between positions on either side of the equator in different regions or seasons, NEI_0 variations lead to hemispherically symmetric modulations of the ITCZ in the annual or zonal mean. Similarly, hemispherically symmetric precipitation variations in double-ITCZ states that symmetrically straddle the equator and are associated with negative NEI_0 are related to NEI_0 variations [Bischoff and Schneider, 2016].

2.2. Indices

To quantify the hemispherically antisymmetric component of the tropical precipitation distribution, we use the tropical precipitation asymmetry index A_p [Hwang and Frierson, 2013]

$$A_p = (\bar{P}_{0-20^\circ N} - \bar{P}_{20^\circ S-0}) / \bar{P}_{20^\circ S-20^\circ N}, \quad (2)$$

where \bar{P} denotes the zonal mean precipitation and $(\cdot)_{\phi_1-\phi_2}$ denotes an area-weighted mean between latitudes ϕ_1 and ϕ_2 . To quantify the hemispherically symmetric component of the tropical precipitation distribution, we use the equatorial precipitation index E_p ,

$$E_p = \frac{\bar{P}_{2^\circ S-2^\circ N}}{\bar{P}_{20^\circ S-20^\circ N}} - 1. \quad (3)$$

In double-ITCZ states that straddle the equator and in which the equatorial precipitation vanishes, E_p assumes its lower bound $E_p = -1$. If tropical precipitation has a uniform distribution, $E_p = 0$. The more strongly peaked tropical precipitation is on the equator, the larger E_p . The absolute values of A_p and E_p are sensitive to the choice of normalization ($\bar{P}_{20^\circ S-20^\circ N}$), but their relative variations across models are not (see supporting information). The corresponding annual mean values of A_p and E_p for the CMIP5 models are given in Table S1, in which models are ordered according to decreasing A_p . It is evident that models produce a wide variety of precipitation indices A_p and E_p .

2.3. Data

We use monthly data from historical simulations of 31 CMIP5 models (Table S1). Only the first realization of ensembles for each model is used. Simulated and observational data were interpolated to a $1^\circ \times 1^\circ$ horizontal grid, and their monthly climatologies were calculated for the years 1979–2004. Data retrieval and analysis were performed using GOAT (Geophysical Observation Analysis Tool, <http://www.goat-geo.org>).

As precipitation data we use the Global Precipitation Climatology Project (GPCP) data [Adler et al., 2003]. We obtained similar results with precipitation data from the Climate Prediction Center (CPC) merged analysis precipitation (CMAP) product [Xie and Arkin, 1996] and from the European Center for Medium-Range Weather Forecasts (ECMWF) Interim Reanalysis [Dee et al., 2011] (hereafter referred to as ERAI).

To calculate the atmospheric energy budget, we use monthly column-integrated ERAI energy fluxes, including a barotropic mass flux correction [Trenberth, 1997; Trenberth and Fasullo, 2012], derived from four times daily data at native reanalysis model resolution (see www.cgd.ucar.edu/cas/catalog/newbudgets/ for details). Because the ERAI radiative budgets are affected by systematic errors [Trenberth et al., 2001], we use the climatological mean (2001–2014) of radiative fluxes from the Clouds and the Earth's Radiant Energy System (CERES) Energy Balanced and Filled (EBAF) data [Wielicki et al., 1996; Loeb et al., 2009]. However, because the period of the ERAI climatology (1979–2004) is dominated by strong El Niño events, whereas the period of the available CERES climatology (2001–2014) is dominated by strong La Niña events, the surface and top-of-atmosphere (TOA) energy fluxes derived from these data sets may include offsets ($\sim 2 \text{ W m}^{-2}$) relative to the CMIP5 ensemble mean, in which the simulated natural El Niño–Southern Oscillation variability is closer to being averaged out.

We calculate annual mean ERAI NEI from the divergence of the atmospheric energy transport (i.e., we assume that energy storage vanishes in the annual mean). These fluxes were found to be more consistent with NEI calculated using CERES data (with a bias $\sim 2 \text{ W m}^{-2}$ [Adam et al., 2016]) than NEI calculated as a residual of

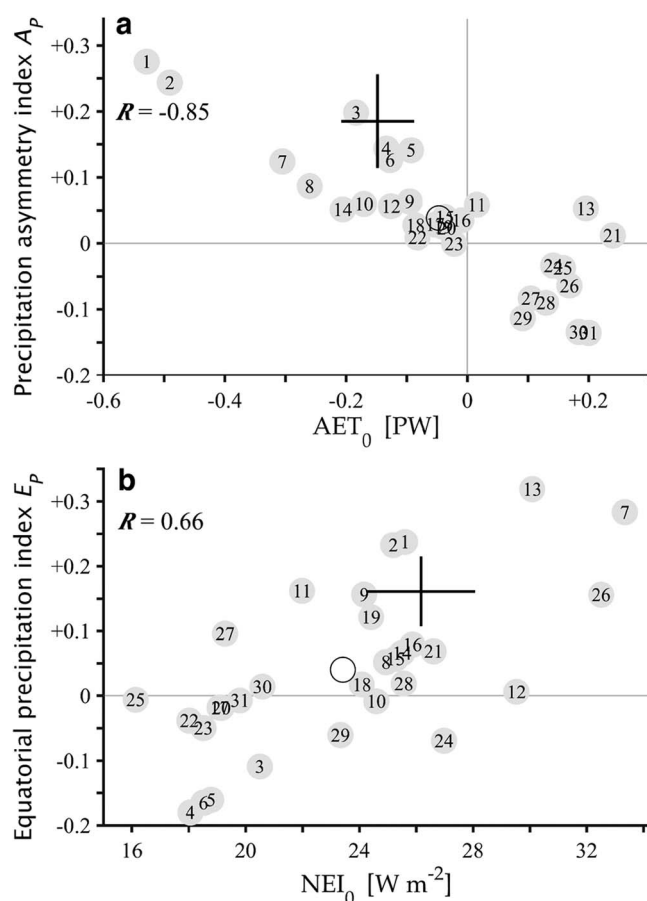


Figure 2. (a) Relation of the annual mean tropical precipitation asymmetry index A_p and cross-equatorial atmospheric energy transport AET_0 . (b) Relation of the annual mean equatorial precipitation index E_p and the equatorial atmospheric net energy input NEI_0 . CMIP5 models are numbered from largest to smallest A_p (Table S1). Ensemble means are shown as open circles, and the observed values (ERA-Interim for energetic quantities and GPCP for precipitation) are shown as bars, whose length corresponds to one standard deviation of interannual variations ($A_p = 0.185 \pm 0.071$, $AET_0 = -0.15 \pm 0.06$ PW and $E_p = 0.161 \pm 0.054$, $NEI_0 = 26.2 \pm 1.9$ W m⁻²).

precipitation in the NH in the present climate (Figure 1a); the multimodel ensemble mean $A_p = 0.04$ is smaller than the observed A_p , because of the excessive precipitation in the southern tropics in the simulations. The observed annual mean E_p is 0.161, the net result of positive contributions over the Maritime Continent and Indian Ocean (where precipitation peaks near the equator) and negative contributions from the weak precipitation in the eastern Pacific and Atlantic cold tongues. The ensemble mean $E_p = 0.038$ is also smaller than the observed E_p , indicating a less equatorially peaked precipitation distribution in the simulations than is observed.

The correlation coefficient of precipitation variations across models with the indices A_p and E_p is shown as a function of latitude in Figures 1b and 1c. The index A_p correlates with hemispherically antisymmetric intermodel variations in the deep tropics (equatorward of $\sim 15^\circ$). The index E_p correlates with hemispherically symmetric intermodel variations within $\sim 30^\circ$ latitude; however, it also correlates with some hemispherically antisymmetric variations, such as a SH precipitation peak that is farther poleward than the NH peak—an antisymmetric variation that is often associated with symmetrically reduced precipitation around the equator [Li and Xie, 2014]. Hence, the two indices indeed characterize different components of annual mean and zonal mean precipitation variations in the vicinity of the ITCZ.

uncertain terms in the energy budgets of the ERA-Interim reanalysis [Trenberth et al., 2001]. We calculate CMIP5 NEI directly from the TOA net shortwave and longwave radiative energy fluxes and from the net shortwave and longwave radiative energy and sensible and latent heat fluxes at the surface. Because of the large equatorial gradients of ocean energy uptake, particularly in the eastern Pacific, NEI values are sensitive to the meridional boundaries of averaging. To obtain the equatorial NEI and AET_0 from ERA-Interim, we average NEI and AET between 5° S and 5° N; NEI from the climate models is obtained in the same way. (The precise choice of averaging region does not affect our results qualitatively; see supporting information.) Because atmospheric energy fluxes with sufficient temporal resolution to include eddy fluxes are not available for all climate models, we calculate CMIP5 AET_0 values as half the difference between the SH and NH integrated atmospheric NEI. The estimated uncertainty in ERA-Interim AET_0 is ~ 0.2 PW [Fasullo and Trenberth, 2008].

3. Results

The meridional distribution of the annual mean and zonal mean tropical precipitation varies substantially across CMIP5 models and has significant hemispherically symmetric and antisymmetric biases (Figure 1a) [Lin, 2007; Li and Xie, 2014]. The observed annual mean A_p is 0.185, consistent with excess

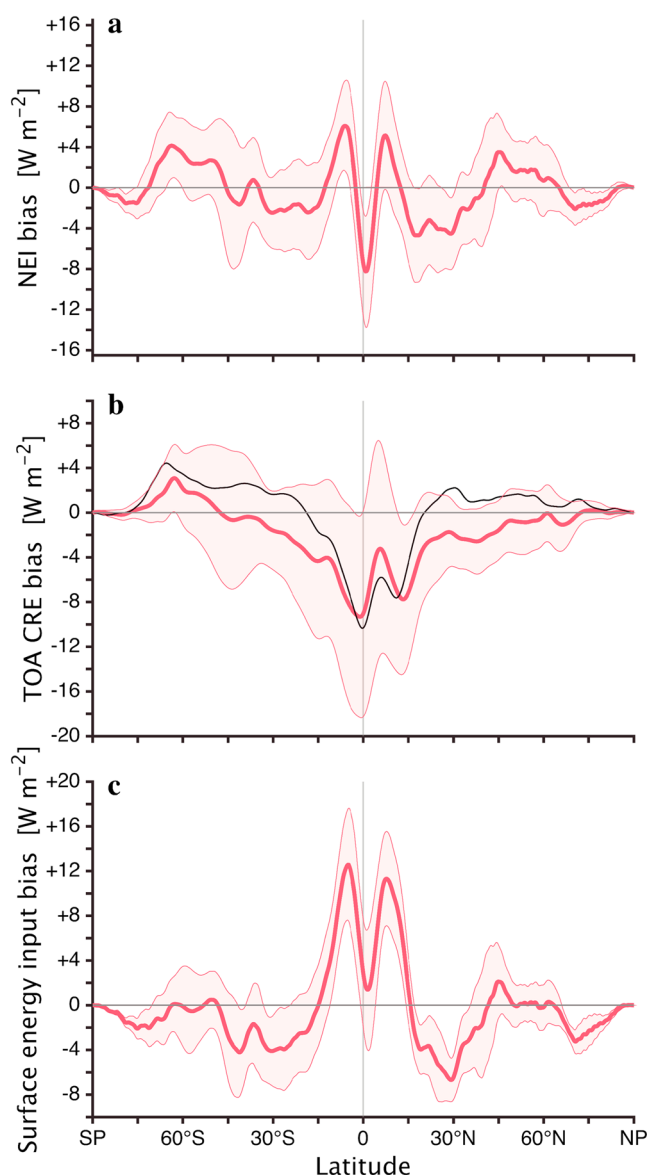


Figure 3. Meridional dependence of the annual mean and zonal mean CMIP5 model bias (i.e., the difference between modeled and observed values) in (a) atmospheric net energy input NEI, (b) net top-of-atmosphere (TOA) radiative input (black) and cloud radiative effect (CRE, red), and (c) surface energy input into the atmosphere. All fluxes are area weighted (i.e., multiplied by the cosine of latitude). The shading indicates one intermodel standard deviation. Observed values are derived from ERAI for NEI, from CERES for TOA radiative fluxes, and from the difference between ERAI NEI and CERES TOA radiative fluxes for surface energy input.

and NEI_0 in the models, we examine the meridional distribution of model biases in NEI. (AET_0 is proportional to the difference in NEI integrated over the two hemispheres, so biases in it can be inferred from NEI biases.) Figure 3 shows the area-weighted zonal mean biases in NEI (Figure 3a), decomposed into biases due to TOA cloud radiative effects (CREs, the difference between total and clear-sky radiative fluxes; Figure 3b) and due to surface energy fluxes (Figure 3c). (Because shortwave and longwave CREs nearly balance at the ITCZ, we use total CRE in Figure 3b to minimize the effect of CRE biases that are induced by biases in the ITCZ position.) Differences in CREs among models dominate the intermodel spread of the tropical NEI bias (Figure 3b)

Consistent with the theoretical expectations from equation (1), A_p is strongly negatively correlated ($R = -0.85$) with cross-equatorial atmospheric energy transport AET_0 (Figure 2a), as was already shown by Hwang and Frierson [2013]. The correlation between A_p and equatorial net energy input NEI_0 is insignificant (not shown) because the fractional intermodel variations in NEI_0 (Figure 2b) are much smaller than the fractional intermodel variations in AET_0 (Figure 2a). This, however, is not the case for temporal variations. For example, interannual variations in NEI_0 are generally not negligible compared with interannual variations in AET_0 in their impact on ITCZ shifts [Adam *et al.*, 2016].

Likewise consistent with the theoretical expectations, a weaker yet clear relation ($R = 0.66$) exists between E_p and NEI_0 (Figure 2b). By contrast, the correlation between E_p and AET_0 is insignificant. (Because the uncertainty in the observations is poorly known, we use one standard deviation of observed interannual variations to indicate the variations of observed quantities, for comparison with those in simulations.) The positive correlation of E_p and NEI_0 (Figure 2b) is consistent with hemispherically symmetric precipitation variations (Figure 1c). Increased NEI_0 is associated with equatorward shifts of precipitation and hence increased precipitation at the equator; decreased NEI_0 is associated with poleward shifts of the ITCZ where and when it is displaced off the equator. It is also associated with more frequent double-ITCZ states.

The correlations between A_p and E_p and those between AET_0 and NEI_0 are insignificant, suggesting that the processes controlling the hemispherically symmetric and antisymmetric variations are not strongly related. To identify processes that may give rise to biases in AET_0

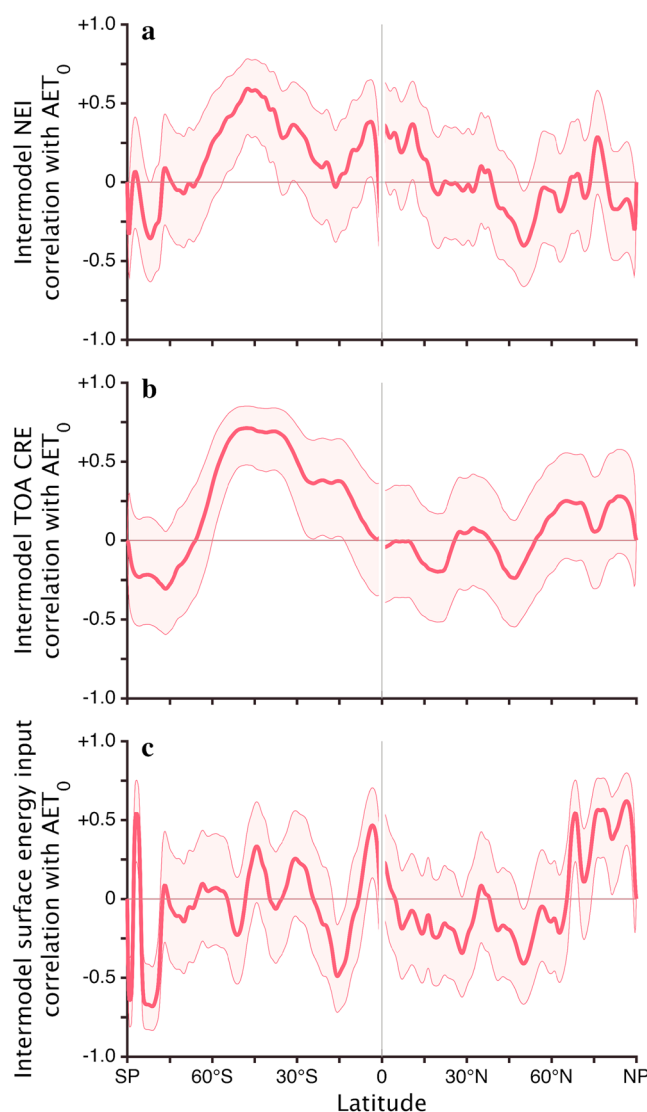


Figure 4. Meridional dependence of the (Pearson) correlation coefficient (shading indicates 95% confidence bounds) between CMIP5 annual mean and zonal mean cross-equatorial atmospheric energy transport AET_0 and (a) atmospheric net energy input NEI, (b) top-of-atmosphere (TOA) cloud radiative effect (CRE), and (c) surface energy input. The sign of the correlation coefficient is reversed in the NH so that positive anomalies in both hemispheres are related to positive anomalies in AET_0 .

model variations in precipitation, we examine the correlation coefficient between intermodel variations in AET_0 and NEI as a function of latitude (Figure 4). As in Figure 3, we decompose NEI variations across models (Figure 4a) into TOA CRE (Figure 4b) and surface energy input (Figure 4c). (The confidence bounds in Figure 4 underestimate the true confidence intervals, because they are based on t statistics, but the lack of independence among the climate models implies that the effective sample size is smaller than the total number of models used in the t statistic.) The sign of the correlation coefficient is reversed in the NH so that positive correlations in both hemispheres are associated with positive AET_0 anomalies. The only NEI variations that are robustly associated across models with variations in AET_0 are those in the SH, which are primarily driven by CRE variations (Figure 4b) [Li and Xie, 2012]. These CRE variations do not appear to be confined to biases in Southern Ocean clouds [cf. Hwang and Frierson, 2013]; rather, the associated cloud biases span the tropics and the midlatitudes, with maximal correlation with AET_0 in the subtropics and midlatitudes. As also shown by

[Li and Xie, 2012]. Increased short-wave reflection by low-level tropical clouds (i.e., a negative TOA CRE bias; Figure 3b) is approximately balanced by surface energy flux biases (Figure 3c) [Li and Xie, 2012]. The residual NEI biases near the equator are associated primarily with too cold, too narrow, and too elongated eastern Pacific cold tongues [e.g., Li and Xie, 2014], which result in surface energy flux biases that reduce NEI near the equator and increased it off the equator (Figure 3a) [Li and Xie, 2012]. The biases have an equatorially symmetric component, but they are not exactly symmetric. The negative bias peaks north of the equator, while the off-equatorial warm bias is larger in the SH [Li and Xie, 2014].

The negative biases in the NH tropics and subtropics arise from Atlantic Meridional Overturning Circulations (AMOCs) that are, on average, too weak in CMIP5 models [Wang et al., 2014]. The negative surface energy input bias in the SH tropics is strongest in the Indian Ocean; it is likely related to biases in ocean-atmosphere coupling there [e.g., Li et al., 2015]. A weak positive bias exists in the SH extratropics due to insufficient reflection by low-level clouds over the Southern Ocean [Hwang and Frierson, 2013; Kay et al., 2016]. Misrepresentation of Antarctic [e.g., Previdi et al., 2015] and Arctic [e.g., Stroeve et al., 2012] sea ice extent may also produce significant clear-sky shortwave reflection biases. However, such biases are not clearly evident in the TOA energy flux bias derived from the CERES data set (Figure 3b, black line).

To identify processes that contribute to hemispherically antisymmetric inter-

Li and Xie [2014], surface energy fluxes are not significantly related to the spread in the asymmetric aspects of the double-ITCZ bias among models. This points to SH tropical and midlatitude cloud variations across models being responsible for AET_0 variations and the associated variations in the tropical precipitation asymmetry index A_p . Similarly, biases in tropical clouds (Figures 3b and 4b) and ocean energy uptake (Figures 3c and 4c) may also be responsible for NEI_0 biases and the associated variations in the equatorial precipitation index E_p .

4. Discussion and Conclusions

Tropical precipitation biases and intermodel variations among coupled climate models (Figure 1a) have hemispherically antisymmetric and symmetric components, which are well characterized by the tropical precipitation asymmetry index A_p (Figure 1b) and the equatorial precipitation index E_p (Figure 1c). Consistent with the first-order arguments relating the position of the ITCZ and energy flux equator to terms in the atmospheric energy balance, we find that hemispherically antisymmetric precipitation biases are primarily related to the cross-equatorial atmospheric energy transport AET_0 (Figure 2a), consistent with *Hwang and Frierson* [2013]; hemispherically symmetric biases are more closely related to the atmospheric net energy input near the equator NEI_0 (Figure 2b).

A negative bias in the CMIP5 NEI_0 ensemble mean (Figure 2b) results from biases in ocean heat transport, surface heat fluxes, and cloud radiative effects [*Li and Xie*, 2012] near the equator. By contrast, CMIP5 models exhibit positive AET_0 biases which are not easily related to NEI biases in a specific region (Figures 3 and 4). They correlate with NEI biases in a broad swath of the SH tropics and midlatitudes. NEI biases in specific latitude bands (e.g., over the Southern Ocean) cannot uniquely be associated with AET_0 biases because local biases may be compensated in their effect on AET_0 biases through opposing biases in other latitude bands [e.g., *Nam et al.*, 2012; *Kay et al.*, 2016] or through a partially compensating ocean energy transport response [*Hawcroft et al.*, 2016].

Positive AET_0 biases are consistent with positive NEI biases in the Southern Ocean due to weak shortwave reflection by low-level clouds [e.g., *Hwang and Frierson*, 2013] but also with negative NEI biases in the NH subtropics and extratropics (related to AMOC biases [*Wang et al.*, 2014]), as well as NEI biases in the deep tropics. However, Southern Ocean and AMOC biases may themselves be related [*Wang et al.*, 2014], making it difficult to consider the effect of either bias on AET_0 independently.

Similarly, deep tropical NEI biases may be a result of the double-ITCZ bias, rather than a cause of it. However, if they are induced by the double-ITCZ bias, these biases imply a positive feedback, whereby positive AET_0 anomalies (driven by, for example, the Southern Ocean shortwave bias or a weaker AMOC) are reinforced by the induced NEI anomalies in the deep tropics. The evidence for such positive cloud feedbacks on ITCZ position is mixed [*Li and Xie*, 2014; *Voigt et al.*, 2014]. Since NEI biases in the deep tropics are directly related to the symmetric aspects of the double-ITCZ bias, and since they may also account for some antisymmetric aspects of the bias, the study of NEI biases in the deep tropics is critical for understanding the double-ITCZ bias.

The interpretation of biases in the atmospheric energy budget of climate models is limited by uncertainty in the observational budgets [*Trenberth et al.*, 2001]. Nonetheless, the correspondence between the NEI biases shown here and known CMIP5 biases [*Flato et al.*, 2013] raises confidence in our results. Further examination of the zonally asymmetric and seasonally varying aspects of tropical precipitation and of the atmospheric energy budget of climate models may provide additional information regarding the origin of ITCZ biases.

Acknowledgments

We thank Michael Byrne for his helpful comments. We thank the National Center for Atmospheric Research (NCAR) Climate and Global Dynamics Laboratory (CGD) for providing the ERA-Interim energy budget products. This research was supported by grants from the Swiss National Science Foundation and the U.S. National Science Foundation (grant AGS-1049201).

References

- Abernathy, R. P., and C. Wortham (2015), Phase speed cross spectra of eddy heat fluxes in the Pacific, *J. Phys. Oceanogr.*, *45*, 1285–1301, doi:10.1175/JPO-D-14-0160.1.
- Adam, O., T. Bischoff, and T. Schneider (2016), Seasonal and interannual variations of the energy flux equator and ITCZ. Part I: Zonally averaged ITCZ position, *J. Clim.*, *29*(9), 3219–3230, doi:10.1175/JCLI-D-15-0512.1.
- Adler, R. F., et al. (2003), The version 2 Global Precipitation Climatology Project (GPCP) monthly precipitation analysis (1979–present), *J. Hydrometeorol.*, *4*, 1147–1167, doi:10.1175/1525-7541(2003)004<1147:TVGPCP>2.0.CO;2.
- Bischoff, T., and T. Schneider (2014), Energetic constraints on the position of the Intertropical Convergence Zone, *J. Clim.*, *27*(13), 4937–4951, doi:10.1175/JCLI-D-13-00650.1.
- Bischoff, T., and T. Schneider (2016), The equatorial energy balance, ITCZ position, and double ITCZ bifurcations, *J. Clim.*, *29*(8), 2997–3013, doi:10.1175/JCLI-D-15-0328.1.
- Broccoli, A. J., K. A. Dahl, and R. J. Stouffer (2006), Response of the ITCZ to Northern Hemisphere cooling, *Geophys. Res. Lett.*, *33*, L01702, doi:10.1029/2005GL024546.

- Chiang, J. C. H., and A. R. Friedman (2012), Extratropical cooling, interhemispheric thermal gradients, and tropical climate change, *Annu. Rev. Earth Planet. Sci.*, **40**, 383–412.
- Chiang, J. C. H., and C. M. Bitz (2005), Influence of high latitude ice cover on the marine Intertropical Convergence Zone, *Clim. Dyn.*, **25**(5), 477–496, doi:10.1007/s00382-005-0040-5.
- Dee, D. P., et al. (2011), The ERA-Interim reanalysis: Configuration and performance of the data assimilation system, *Q. J. R. Meteorol. Soc.*, **137**, 553–597, doi:10.1002/qj.828.
- Delworth, T. L., et al. (2012), Simulated climate change in the GFDL CM2.5 high-resolution coupled climate model, *J. Clim.*, **25**, 2755–2781, doi:10.1175/JCLI-D-11-00316.1.
- Donohoe, A., J. Marshall, D. Ferreira, and D. McGee (2013), The relationship between ITCZ location and cross-equatorial atmospheric energy transport: From the seasonal cycle to the Last Glacial Maximum, *J. Clim.*, **26**, 3597–3618, doi:10.1175/JCLI-D-12-00467.1.
- Fasullo, J. T., and K. E. Trenberth (2008), The annual cycle of the energy budget. Part II: Meridional structures and poleward transports, *J. Clim.*, **21**, 2313–2325.
- Flato, G., et al. (2013), Evaluation of climate models, in *Climate Change 2013: The Physical Science Basis. Contribution of Working Group I to the Fifth Assessment Report of the Intergovernmental Panel on Climate Change*, edited by T. F. Stocker et al., Cambridge Univ. Press, Cambridge, U. K. New York.
- Hawcroft, M., J. M. Haywood, M. Collins, A. Jones, A. C. Jones, and G. Stephens (2016), Southern Ocean albedo, inter-hemispheric energy transports and the double ITCZ: Global impacts of biases in a coupled model, *Clim. Dyn.*, **1**–17, doi:10.1007/s00382-016-3205-5.
- Hwang, Y.-T., and D. M. M. Frierson (2013), Link between the double-Intertropical Convergence Zone problem and cloud biases over the Southern Ocean, *Proc. Natl. Acad. Sci. U.S.A.*, **110**, 4935–4940, doi:10.1073/pnas.1213302110.
- Kang, S. M., I. M. Held, D. M. W. Frierson, and M. M. Zhao (2008), The response of the ITCZ to extratropical thermal forcing: Idealized slab-ocean experiments with a GCM, *J. Clim.*, **21**, 3521–3532, doi:10.1175/2007JCLI2146.1.
- Kay, J. E., C. Wall, V. Yettella, B. Medeiros, C. Hannay, P. Caldwell, and C. Bitz (2016), Global climate impacts of fixing the Southern Ocean shortwave radiation bias in the Community Earth System Model (CESM), *J. Clim.*, **29**(12), 4617–4636, doi:10.1175/JCLI-D-15-0358.1.
- Li, G., and S.-P. Xie (2012), Origins of tropical-wide SST biases in CMIP multi-model ensembles, *Geophys. Res. Lett.*, **39**, L22703, doi:10.1029/2012GL053777.
- Li, G., and S.-P. Xie (2014), Tropical biases in CMIP5 multimodel ensemble: The excessive equatorial Pacific cold tongue and double ITCZ problems, *J. Clim.*, **27**, 1765–1780, doi:10.1175/JCLI-D-13-00337.1.
- Li, G., S.-P. Xie, and Y. Du (2015), Climate model errors over the South Indian Ocean thermocline dome and their effect on the basin mode of interannual variability, *J. Clim.*, **28**, 3093–3098, doi:10.1175/JCLI-D-14-00810.1.
- Lin, J.-L. (2007), The double-ITCZ problem in IPCC AR4 coupled GCMs: Ocean–atmosphere feedback analysis, *J. Clim.*, **20**, 4497–4525, doi:10.1175/JCLI4272.1.
- Loeb, N., B. Wielicki, D. Doelling, G. Smith, D. Keyes, S. Kato, N. Manalo-Smith, and T. Wong (2009), Toward optimal closure of the Earth's top-of-atmosphere radiation budget, *J. Clim.*, **22**, 748–766, doi:10.1175/2008JCLI2637.1.
- Marshall, J., A. Donohoe, D. Ferreira, and D. McGee (2014), The ocean's role in setting the mean position of the Intertropical Convergence Zone, *Clim. Dyn.*, **42**, 1967–1979, doi:10.1007/s00382-013-1767-z.
- Mechoso, C. R., et al. (1995), The seasonal cycle over the tropical Pacific in coupled ocean–Atmosphere general circulation models, *Mon. Weather Rev.*, **123**, 2825–2838.
- Nam, C., S. Bony, J.-L. Dufresne, and H. Chepfer (2012), The “too few, too bright” tropical low-cloud problem in CMIP5 models, *Geophys. Res. Lett.*, **39**, L21801, doi:10.1029/2012GL053421.
- Philander, S. G. H., D. Gu, D. Halpern, G. Lambert, N.-C. Lau, T. Li, and R. C. Pacanowski (1996), Why the ITCZ is mostly north of the equator, *J. Clim.*, **9**, 2958–2972.
- Previdi, M., K. L. Smith, and L. M. Polvani (2015), How well do the CMIP5 models simulate the Antarctic atmospheric energy budget?, *J. Clim.*, **28**, 7933–7942, doi:10.1175/JCLI-D-15-0027.1.
- Schneider, T., T. Bischoff, and G. H. Haug (2014), Migrations and dynamics of the Intertropical Convergence Zone, *Nature*, **513**, 45–53, doi:10.1038/nature13636.
- Small, R. J., et al. (2014), A new synoptic scale resolving global climate simulation using the Community Earth System Model, *J. Adv. Model. Earth Syst.*, **6**, 1065–1094, doi:10.1002/2014MS000363.
- Stroeve, J. C., V. Kattsov, A. Barrett, M. Serreze, T. Pavlova, M. Holland, and W. N. Meier (2012), Trends in Arctic sea ice extent from CMIP5, CMIP3 and observations, *Geophys. Res. Lett.*, **39**, L16502, doi:10.1029/2012GL052676.
- Tian, B. (2015), Spread of model climate sensitivity linked to double-Intertropical Convergence Zone bias, *Geophys. Res. Lett.*, **42**, 4133–4141, doi:10.1002/2015GL064119.
- Trenberth, K. E. (1997), Using atmospheric budgets as a constraint on surface fluxes, *J. Clim.*, **10**, 2796–2809, doi:10.1175/1520-0442(1997)010<2796:UABAAC>2.0.CO;2.
- Trenberth, K. E., and J. T. Fasullo (2012), Tracking Earth's energy: From El Niño to global warming, *Surv. Geophys.*, **33**–3, 413–426, doi:10.1007/s10712-011-9150-2.
- Trenberth, K. E., J. M. Caron, and D. P. Stepaniak (2001), The atmospheric energy budget and implications for surface fluxes and ocean heat transports, *Clim. Dyn.*, **17**, 259–276, doi:10.1007/PL00007927.
- Vellinga, M., and R. A. Wood (2002), Global climatic impacts of a collapse of the Atlantic thermohaline circulation, *Clim. Change*, **54**, 251–267, doi:10.1023/A:1016168827653.
- Voigt, A., S. Bony, J.-L. Dufresne, and B. Stevens (2014), The radiative impact of clouds on the shift of the Intertropical Convergence Zone, *Geophys. Res. Lett.*, **41**, 4308–4315, doi:10.1002/2014GL060354.
- Wang, C., L. Zhang, S.-K. Lee, L. Wu, and C. R. Mechoso (2014), A global perspective on CMIP5 climate model biases, *Nat. Clim. Change*, **4**, 2201–2205, doi:10.1038/nclimate2118.
- Wielicki, B. A., B. R. Barkstrom, E. F. Harrison, R. B. Lee III, G. L. Smith, and J. E. Cooper (1996), Clouds and the Earth's Radiant Energy System (CERES): An Earth observing system experiment, *Bull. Am. Meteorol. Soc.*, **77**, 853–868, doi:10.1175/1520-0477(1996)077<0853:CATERE>2.0.CO;2.
- Xie, P., and P. Arkin (1996), Analyses of global monthly precipitation using gauge observations, satellite estimates, and numerical model predictions, *J. Clim.*, **9**, 840–858, doi:10.1175/1520-0442(1996)009<0840:AOGMPU>2.0.CO;2.
- Zhang, X., H. Liu, and M. Zhang (2015), Double ITCZ in coupled ocean-atmosphere models: From CMIP3 to CMIP5, *Geophys. Res. Lett.*, **42**, 8651–8659, doi:10.1002/2015GL065973.